An Automated Methodology for Events Classification in Power Plants Based on DFR Data and Symmetrical Components

Dionatan A. G. Cieslak, * **Heitor J. Tessaro, Miguel Moreto** *

* *PPGEEL - Graduate Program in Electrical Engineering, Federal University of Santa Catarina, UFSC*

Abstract: Digital Fault Recorders (DFR) are valuable devices for power system monitoring since they allow the analysis of electrical quantities and information from the protection system. This paper presents two automated methodologies for event classification in power plants based on the phasor records, thus the same methodologies can be applied to PMU data. Besides the classification of the power units' operational states, the methodologies can also diagnose the causes of forced shutdowns of units based on the analysis of the symmetrical components. The process of fault classification aims to identify distinct events, such as single, double or three-line faults. The paper presents a comparison between pros and cons of the use of a specialist approach, based on fuzzy logic, and a generalist approach, based on convolutional neural networks. The methodologies are tested and evaluated with simulated data, and the validation is performed using real disturbance records. The results demonstrate the feasibility and effectiveness of the proposed methods. The convolutional network approach presented better performance with simulated data, while the fuzzy based approach managed to maintain its accuracy when used to classify real records.

Keywords: Digital Fault Recorder, Fault Classification, Fuzzy Logic, Machine Learning, Symmetrical Components.

1. INTRODUCTION

The increase of monitoring systems, together with the exponential enhancement in computer processing data, has stimulated the development of technologies dedicated to diagnosing electrical power system failures. The Digital Fault Recorders (DFRs) play an important role in these applications. When used in power plants, the DFRs perform the monitoring of the generators' electrical quantities. DFRs have been widely used in the offline analysis of events in power plants, providing information to the engineering analysis staff about disturbances that commonly occur in power systems. A DFR records sampled waveform of voltages and currents signals, as well the status of relays and other digital quantities. When a quantity exceeds a specified trigger or when the status of one or more digital inputs changes, the DFR saves a disturbance record. Consequently, when a disturbance is detected, the record contains pre- and post-disturbance information (Perez, 2010).

The signals in the disturbance record can contain signatures related with the event. In Asman et al. (2020) the authors investigate fault signatures from different roots causes and propose several detection indexes. The use of fault signatures among with classification techniques are frequently employed to automate the analysis of power systems disturbances. Examples of such techniques that are based on fuzzy logic and symmetrical components are presented in Agrawal and Koley (2016); Katyara et al. (2018). Most of the works focus on transmission and distribution systems.

With the advancements and popularization of free-online libraries such as Scikit-learn, PyTorch, TensorFlow, and Keras, artificial intelligence-based techniques are becoming popular. Applications of convolutional sparse autoencoder and deep recurrent neural networks for fault diagnosis in transmission lines are proposed in Chen et al. (2016) and Belagoune et al. (2021) respectively. The transformation of time-series signal in 2D images, instead of the direct use of time-series data, combined with the use of convolutional neural networks may improve the classification accuracy (Miranda et al., 2019). Furthermore, the inclusion of complementary information, as angle shift and the rate of change of frequency when dealing with frequency related events, may improve the classification robustness (Wang et al., 2020).

Considering the power generation systems, it was verified that many events happen in a power plant every day, and each event may result in a new DFR record that must be analyzed (Moreto and Rolim, 2015). Due to the amount of generated data, it is reasonable to apply smart automated techniques to support the analysis. Besides, the data from the rest of the system may not be available for each power plant operator, thus, an event classifier considering only local data may be used. In the context of the aforementioned facts, this paper proposes two classification tools to automate the analysis of disturbances. The proposition of two tools aims to compare and assess the pros and cons

⋆ Corresponding author: dcieslak@utfpr.edu.br

of a specialist technique, based on fuzzy logic, against a generalist technique, based on convolutional neural networks. While the effectiveness of the first one rely on the experience of the operator, the effectiveness of the second one rely on the amount of data available. Both tools aim to classify the events recorded by DFRs installed in power plants. This paper uses long duration phasor records from DFR and symmetrical components, instead of traditional short duration (waveform) records.

2. FUNDAMENTALS OF FUZZY INFERENCE SYSTEMS AND CONVOLUTIONAL NEURAL NETWORKS

2.1 Fuzzy Inference System

A FIS maps the knowledge and model it in order that a set of rules correlate inputs (antecedents) and outputs (consequent) within and conditional structure. Basically, the inputs and outputs are modeled through the concepts of membership functions. Such information is correlated through logical connectives by an inference engine which contains a set of rules, based on expert knowledge of the process (Ross, 2010). In this paper, two Mamdani FIS are designed in order to classify events in a power plant based on symmetrical responsible to separate normal events from abnormal ones (events that force the unit's shutdown). FIS II aims to classify the nature of the disturbance, i.e, the type of the fault. For both inference system, the fuzzy inputs are modeled as geometrical membership functions, based on the common per unit values of electrical quantities. Outputs are modeled based on the singleton concept. The development of the FIS in this paper is based on Skfuzzy, a fuzzy logic toolbox for SciPy.

2.2 Convolutional Neural Network

CNN are neural networks that use convolution instead of matrix multiplication. Each convolutional layer consists of many applications of convolution in parallel, with the objective of extracting the maximum number of features as possible. The basic layer of a CNN contains several kernels, activation functions, and pooling functions Goodfellow et al. (2016). The parallel kernels perform the convolution. The kernels output forms new feature maps, usually with smaller size (Wang et al., 2020). This paper uses the CNN for events classification. To this end, a SoftMax layer is used at the end of the CNN to determine the probability of each sample to belong to each class. Furthermore, max-pooling is used to perform the pooling function, and the rectified linear unit (ReLU) is used as activation function. For the training, it is used the cross entropy loss as the loss function and stochastic gradient descent for updating the weights. The development of the CNN in this paper is based on the PyTorch library.

3. FEATURES AND DATA PREPARATION

The classifiers aim to classify events related to the daily operation of synchronous generators. These events are related to normal operation and forced shutdown scenarios. Tab.1 presents the description and ID of all classes of events considered in this paper. In Tab. 1, THVS means the transformer high voltage side, and TLVS means the transformer low voltage side.

Table 1. Classes of events.

Fuzzy ID	CNN ID	Description
DESE01		Desenergization of the unit
LINC02		Load increase
LDEC03		Load decrease
SHUT04	SPFH04	THVS line-to-ground fault shutdown
	SPFL05	TLVS line-to-ground fault shutdown
	DPFH06	THVS line-to-line fault shutdown
	DPFL07	TLVS line-to-line fault shutdown
	DGFH08	THVS double-line-to-ground fault shutdown
	DGFL09	TLVS double-line-to-ground fault shutdown
	SGFH10	THVS simetric-to-ground fault shutdown
	SGFL11	TLVS simetric-to-ground fault shutdown
NOOP05		THVS temporary line-to-ground fault
		THVS temporary line-to-line fault
		THVS temporary double-line-to-ground fault
		THVS temporary simetric-to-ground fault

Class DESE01 represents an operational behavior that is described by the reducing of the voltage from nominal values up to zero while the unit has no loading. Classes LINC02 and LDEC03 are characterized by the voltage maintenance near to nominal values and the increase or decrease of current values, since the initial values are not null. Class SHUT04 corresponds to a load rejection, which means that the current reduces from its values to zero as well as voltage. Finally, class NOOP05 corresponds to normal operation of the unit, that is, both current and voltage still the same all over the record. In this paper, normal operation is related to external faults (events that do not cause the breaker's trigger).

One of the classifiers proposed in this paper uses a neural network. The training process of neural networks for classification purpose demands a vast number of examples to achieve satisfactory results. Therefore, due to the limitation of available real data records from DFRs, in this paper the training and validation process of the CNN uses simulated data. However, it is not the case for the fuzzy based classifier, since it is a specialist system. Consequently, the accuracy of the fuzzy classifier does not rely on the number of data examples, but on the knowledge of the specialist that defines the fuzzy parameters. To provide the simulated data, this paper uses a Simulink system composed by a synchronous machine connected to a slack bus.

3.1 Simulation System

The simulation model used is composed by a three-phase synchronous generator rated 200 MVA, 13.8 kV, FP = 0.92 inductive, connected to a 230 kV, 10.000 MVA network through a Δ-wye 210 MVA transformer, as shown in Fig. 1. The synchronous generator is driven by a hydraulic turbine, and operates with speed and voltage regulators. The simulated scenarios related to the shutdown or desenergization of the synchronous generator result in the disconnection of the generator from the system by a circuit breaker.

To ensure data variability for all type of events, each simulation uses a different operating point for the synchronous generator. Previous to each event simulation, a randomly operating point is selected, as well as other

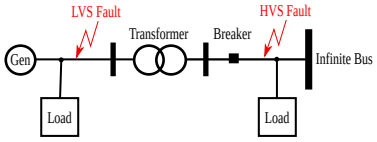

Figure 1. Single-line diagram of the simulation system.

simulation parameters. Therefore, for each simulation first the parameters are selected considering its range, next, the system operating point is determined by solving the power flow, and then the event is simulated. Furthermore, in fault events related to line-to-ground, line-to-line and double-line-to-ground, all combination of the phases related to the faults are equally used.

The list of variable parameters used in the simulation and their ranges are: synchronous generator power level varying from 0.3 up to 1 p.u; power factor from 0.9 to 1 p.u; fault time interval (that causes shutdown) from 0.2 to 1.5 s; fault time interval (temporary faults) from 0.05 to 0.3 s and fault resistance from 10^{-3} to $10^{-1}\,\Omega$.

The event classifiers use the measured current and voltage phasors of the generator terminals as the input data. The DFR saved record contains pre- and post-disturbance information. This paper considers that the DFR samples the measurement signals at 60 Hz, and each record stores 240 s of operation data, totalizing 14400 samples per record. Besides, all simulations consider that the event occurs at 34 s.

The DFR record contains the voltage and currents signals in p.u.. After the DFR saves a record, the symmetrical components of the currents and voltages are calculated, totalizing six signals. The proposed classifiers just use the magnitude of the symmetrical components, therefore, the phases are dropped.

3.2 Data preparation for the FIS

Once the symmetrical components of current and voltage are calculated, the record is segmented into pre, during and post-transient. Magnitude mean values for each component at each segment are determined, and the features are then obtained as: $V_{pre}^{(0,1,2)}$, $V_{tra}^{(0,1,2)}$, $V_{pos}^{(0,1,2)}$, $I_{pre}^{(0,1,2)}$, $I_{tra}^{(0,1,2)}$ and $I_{pos}^{(0,1,2)}$. The segmentation window can be observed in Fig. 2, where the shadowed area represents the transient instant (in detail), all the samples at the left of the window represent the pre-transient quantities and all the samples, at the right, represent the post-transient quantities.

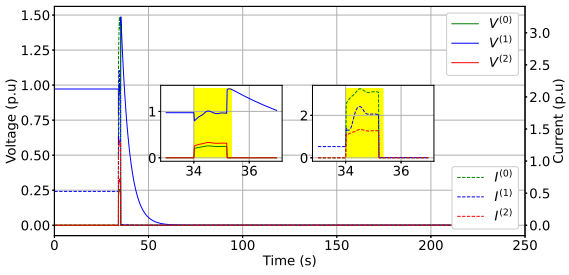

Figure 2. Symmetrical components of a segmented record. Typical behavior of a SPFL05 event.

FIS I, called *Event Classifier*, uses positive sequence current and voltage from pre- and post-transient segments, while FIS II, called *Fault Classifier*, uses, basically, zero and negative components of currents and voltages from transient segment.

3.3 FIS Architecture

All the inputs from the FIS I are shown in Tab. 2 (where NU means a Null, IN means an Intermediate and NO a Nominal membership function). Based on the power unit's operating ranges, the fuzzy inputs are modeled using trapezoidal shapes. Only one event corresponds to a situation which is not related to normal operational procedures (SHUT04 in Tab. 1). In this way, the occurrence of this event represents a probable contingency, so, every time FIS I detect a forced shutdown, automatically, a second fuzzy inference system (FIS II) is initialized. Most of the fault detection or classification of DFR data are based on short duration records. This methodology uses the same long duration record to classify the nature of the event that causes a force shutdown in the machine.

FIS II is able to classify symmetric and unsymmetrical faults. The occurrence of unsymmetrical (single, double and double-grounded-phase) faults is way more common than symmetrical (three-grounded-phase) ones. During the occurrence of a fault and at the point of the fault, each one of them has a particular behavior (as known as fault signature) based on the relations of the fault currents and voltages from the classical short circuit theory Kundur (1994); Saadat (1999).

Based on these relations, a helpful action is to concatenate them into a unique variable (in order to simplify the fuzzy modeling of FIS II). Thus, we propose two factors (called Negative Current Unbalanced Factor - ψ_I and Negative Voltage Unbalanced Factor - ψ_V) that gather unsymmetrical faults characteristics, allowing the simplicity and effectiveness of FIS II:

$$\psi_I = \frac{I_{tra}^{(0)}}{I_{tra}^{(2)}} \qquad \psi_V = \frac{V_{tra}^{(0)}}{V_{tra}^{(2)}} \tag{1}$$

The observation of the behavior of the unbalanced factors for all the simulated fault cases helps the membership functions design. Tab. 2 also shows all the FIS II inputs (where NU means a Null, LO means a Low, IN means an Intermediate and HI means a High membership function). Once is not possible to observe these signatures in symmetrical faults, FIS II also considers the magnitude of $V_{tra}^{(2)}$. All the outputs classes from FIS I and II (column Fuzzy ID in Tab. 1) are modeled based on singletons.

The rules of the FIS I and FIS II are shown in Tab. 3. As an example, when the second rule is activated, the record presents a reduced from nominal values to null values of voltage and the maintenance of the current in null values, so, the expected output of the inference is that the event class is 100% DESE01.

Table 2. Inputs membership function parameters.

Trapezoid Parameters	FIS I									FIS II									
	$V_{pre}^{(1)}$, $V_{pre}^{(1)}$			$I_{pre}^{(1)}$, $I_{pos}^{(1)}$			$\Delta I^{(1)}$			ψ_I				ψ_V				$V_{tra}^{(2)}$	
	NU	IN	NO	NU	IN	NO	NE	NU	PO	NU	LO	IN	HI	NU	LO	IN	HI	LO	HI
A	0	0.15	0.65	0	0.2	0.6	-1.1	-0.05	0.01	0	0.1	2	2.5	0	0.1	0.7	0.8	0	0.01
B	0	0.25	0.75	0	0.3	0.7	-1.1	-0.01	0.05	0	0.15	2.2	2.6	0	0.15	0.75	0.85	0	0.02
C	0.15	0.65	1.2	0.2	0.6	1.2	-0.05	0.01	1.1	0.1	0.7	2.5	3.2	0.1	0.7	0.8	1.2	0.01	1.2
D	0.25	0.75	1.2	0.3	0.7	1.2	-0.01	0.05	1.1	0.15	0.75	2.6	3.2	0.15	0.75	0.85	1.2	0.02	1.2

Table 3. FIS I and II - set of rules

FIS I																FIS II							
Rule	1	2	3	4	5	6	7	8	9	10	11	12	13	14	15	Rule	1	2	3	4	5	6	7
$V_{pre}^{(1)}$	NO	NO	NO	NO	NO	NO	NO	NO	NO	NO	NO	NO	NO	NO	NO	ψ_I	IN	NU	LO	LO	HI	HI	NU
$V_{pos}^{(1)}$	NU	NU	NO	NO	NO	NO	NO	NO	NO	NO	NU	NU	NO	NO	NO	ψ_V	IN	NU	LO	HI	LO	HI	NU
$I_{pre}^{(1)}$	NU	NU	NO	IN	IN	NU	NO	NO	IN	IN	NO	IN	NO	IN	NU	$V_{tra}^{(2)}$	HI	HI	HI	HI	HI	HI	LO
$I_{pos}^{(1)}$	NU	NU	NO	IN	NO	IN	NO	IN	IN	NU	NU	NU	NO	IN	NU	Event	SPFH04 SPFL05	DPFH06 DPFL07	DGFH08 DGFL09				SGFH10 SGFL11
$\Delta I^{(1)}$	NU	NE	PO	PO	PO	PO	NE	NE	NE	NE	NE	NE	NU	NU	NU								
Event	DESE01		LINC02				LDEC03				SHUT04		NOOP05										

3.4 Data preparation for the CNN

The first preparation process for the CNN involves saturation and discretization of the symmetrical components. First, the symmetrical components from the simulated records are saturated, considering the limits of 1.5 p.u. for the voltage and 2 p.u. for the current. Then, the six saturated symmetrical components are discretized into 256 levels. As a result of the discretization into 256 levels described before, each matrix may be seen as a gray-scale image.

To be used as inputs by the CNN, the six saturated symmetrical components need to be converted to image formats or, in other words, each vector must be converted to a two-dimensional matrix. Each symmetrical components record contains 14400 samples, thereby, each one is reshaped in a 120×120 matrix. Therefore, each DFR record results in six 120x120 matrices.

3.5 CNN Architecture

In this paper, three convolutional layers and three fully connected layers constitutes the basic CNN structure. Tab. 4 demonstrates the complete structure of the CNN model, and the size of inputs and outputs of each layer. In Tab. 4, k is the kernel size, f is the number of the features maps, s is the stride, p is the probability of an element to be zeroed, *in* is the input neuron number, and *out* is the output neuron number. The Activation layers perform the activation function, and the Flatten layer transforms the inputs into a flat vector used as input to the first fully connected layer, named as Linear.

Table 4. CNN structure.

Input size	Operation performed by the layer	Output size
120x120x6	Conv1 ($k = 6$, $f = 36$, $s = 2$)	58x58x36
58x58x36	Activation1	58x58x36
58x58x36	MaxPool1 ($k = 2$, $s = 2$)	29x29x36
29x29x36	BatchNorm1 ($f = 36$)	29x29x36
29x29x36	Conv2 ($k = 6$, $f = 50$, $s = 1$)	24x24x50
24x24x50	Activation2	24x24x50
24x24x50	MaxPool2 ($k = 2$, $s = 2$)	12x12x50
12x12x50	BatchNorm2 ($f = 50$)	12x12x50
12x12x50	Conv3 ($k = 7$, $f = 100$, $s = 1$)	6x6x100
6x6x100	Activation3	6x6x100
6x6x100	MaxPool3 ($k = 2$, $s = 2$)	3x3x100
3x3x100	BatchNorm3 ($f = 100$)	3x3x100
3x3x100	Flatten	900x1
900x1	Linear1 ($in = 900$, $out = 300$)	300x1
300x1	Activation4	300x1
300x1	Dropout1 ($p = 0.3$)	300x1
300x1	Linear2 ($in = 300$, $out = 50$)	50x1
50x1	Activation5	50x1
50x1	Dropout2 ($p = 0.3$)	50x1
50x1	Linear3 ($in = 50$, $out = 15$)	15x1

4. RESULTS

This section presents the results obtained using FIS and CNN classifiers for the classes of events presented in Tab. 1. To perform both fuzzy classification and CNN classification training and validation, 300 examples for each class were simulated using the system described previously, shown in Fig. 1, totaling 4500 events. To evaluate the effectiveness of the classifiers, 450 complementary noised examples are used, 30 for each type of event. A white noise with range of ±0.01 p.u. was added to the symmetrical components of these new examples. First, the FIS classifiers results are presented, followed by the results of the CNN considering the simulated data. At the end, a validation of both classifiers is presented using real data.

4.1 FIS classifier

Initially, FIS I and II were modeled and tested with all the 4500 recorded data. FIS I showed an accuracy of 93.8% and FIS II, 97.6%. To present the effectiveness of the FIS I face to the multi-class classification problem of 5 classes, Fig. 3a shows the confusion matrix. It is possible to see that all the classes presented some percentage of dubious classification (in particular, classes LINC02 and LDEC03 showed a higher confusion). This fact occurs, basically, due to the adjusts in setting the parameters of the membership functions (in this case, the $\Delta I^{(1)}$ membership functions). Furthermore, once a fuzzy modelling presents a non-strict reasoning since the membership functions maps semantically the crisp values, it is expected that dubious outputs showed up. Nevertheless, even with some degree of confusion, the classifier can be considered satisfactory, with an accuracy of approximately 96%.

The fact the neutral current of the transformer is not recorded implies that the fuzzy classifier could not identify if the fault is located at TLVS or THVS. Moreover, short circuit signatures, from which the unbalanced factors are derived, are fully satisfied only near the fault point. This way, to verify the accuracy of the FIS II, low voltage side fault recorders are evaluated and then, the inference system is applied to the high voltage side fault recorders. Confusion matrices are shown in Fig. 3b and 3c.

The fuzzy classifier based on symmetrical components showed effectiveness facing the multi-class problem (even with dubious conclusions between classes). But for most of the cases, the conclusion was correct, presenting an accuracy of 92.5%. For faults located at the high voltage side, the inference has not performed as well as the low voltage side, with an accuracy of 51.6%. This is expected as the measurement occurs at the terminals of the generator, i.e, low voltage side. So, all the disturbances that occur at the high voltage side do not, necessarily, present the fault signatures that are the kernel for the unbalanced factors due to the transformer Δ-wye connection. As an example, in this case, an event labeled SPFH04 is seen as a DPFL07.

4.2 CNN classifier

Initially, the set of 4500 data records were shuffled and split in training data (80%) and validation data (20%). Mini-batches size of 90 records were used. In the training, this paper uses categorical loss as the loss function and stochastic gradient descent (SGD) as the update function, with learning rate of 0.001, weight decay of 10^{-5}, and momentum of 0.9. At the end of the training process, the accuracy of CNN II for training data was 99.75% and for validation data was 99.92%, totalizing an average accuracy of 99.83%. On the other hand, the best average accuracy was registered at the 39th training epoch, and the network parameters at this point form the CNN I. The accuracy of CNN I for training data was 99.81% and for validation data was 100%, totalizing an average accuracy of 99.9%. Thus, CNN I was selected as the final CNN of the training process.

For a validation purpose and to emulate disturbances in the measurement system, the 450 complementary noised examples were evaluated. To verify the effectiveness of the CNN classifier face to the 12 classes classification problem, Fig. 4 shows the confusion matrix of the results. Due to the use of new noised data, the overall accuracy reduced to 94%. The LINC02 and LDEC03 classes were the ones with the lowest accuracy level. The simulation used to generate the dataset for the CNN training related to the LINC02 and LDEC03 classes considered variable load steps, in which amplitude could be small. Therefore, some load increase/decrease scenarios ended up presenting behavior similar to transitory disturbances (NOOP05). Thus, this similarity resulted in the deterioration of the CNN accuracy face to the new noised data. A complementary reason may be related to the CNN size and training. As the accuracy during the training and validation process reached high level for all classes, it is possible that happened overfitting to these data. However, the CNN accuracy also reached high level for validation data, which is not used for training. Thus, it indicates high similarity between training and validation data, which may not be the case with the noised data.

4.3 Validation with real data

A total of 44 real cases are evaluated. These cases are obtained from DFRs installed in a coal-fired thermal power plant with four generating units (each one of 24 MVA and 6 kV). Fig. 5 presents a real record related to a forced shutdown. In this event a short circuit at the high voltage winding of the generator's transformer started when the cable that connected the surge arrester touched the ground after its explosion. Therefore, the shown case belongs to the SPFH04 class.

The FIS I outcome is SHUT04 (with no percentage in other classes). Once the classification is the class SHUT04, the FIS II is performed and its outcome is 100% for DPFH06/DPFL07 (the output does not distinguish if the fault is located at the LVS or the HVS). Once the operator's report considers the disturbance as a single-line short circuit at the high voltage winding and taking the transformer connection into account, the disturbance is seen as a double-line fault at the low voltage side, so the output of FIS II is accurate, classifying the disturbance as a DPFL07.

The CNN output for the Fig. 5 data was 64.2% for SPFH04, 10.5 % for DGFH08, 10.3% for SPFL05, and the remaining percentage distributed among the other classes. Therefore, the CNN correctly classified the record. Due to the lack of information related to the shutdown cases, all faults followed by a shutdown are grouped to the same SHUT04 class. Thus, the 44 real records are related to the classes DESE01, LINC02, LDEC03, SHUT04, and NOOP05. NOOP05 has 30 examples. Considering the real cases, the fuzzy classifier presented an accuracy of 95.45%. On the other hand, the CNN presented an accuracy of 79.59%.

The fuzzy classifier classified most of the real records accurately. The misclassification occurred with classes DESE01 and SHUT04. The main reason for this is related to the limits of the membership functions, as example, the values that define what is an intermediate operational value and a nominal operational value. Nevertheless, the outcome of FIS I and II are satisfactory and the non-strict output is a common characteristic when dealing with fuzzy sets. The majority of the misclassified cases by the CNN were of DESE01 class. This scenario is similar to the misclassification related to the noised data. However, now the DESE01 cases were seen as fault disturbances. It happens due to the discrepancy between the simulated and real data. The simulated data shows clean signal, with the current becoming null immediately, substantially different of some real cases.

5. CONCLUSIONS

This paper proposed two classifiers for determining event types in synchronous generator operation based on DFR records. Both classifiers achieved accuracy levels above 93.8% for event and TLVS fault classification using 4500 training examples. The addition of measurement noise did not significantly affect classifier effectiveness. However,

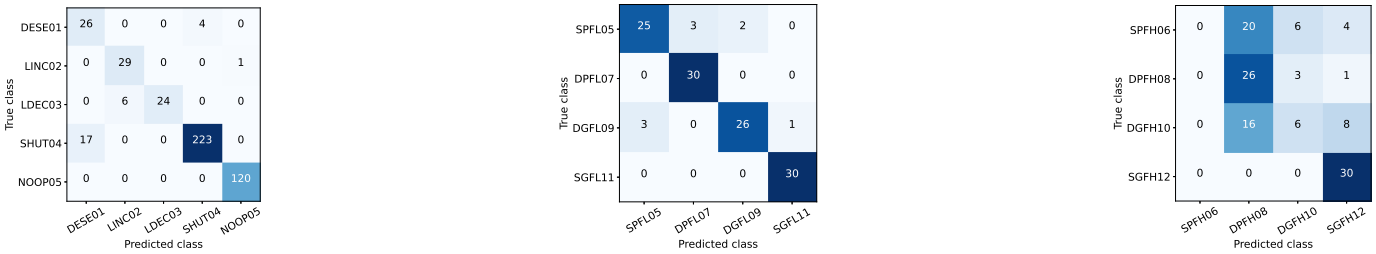

(a) FIS I (b) FIS II - TLVS faults (c) FIS II - THVS faults

Figure 3. Confusion matrices of FIS I and FIS II.

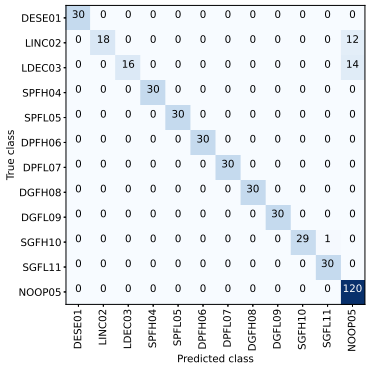

Figure 4. Confusion matrix of CNN.

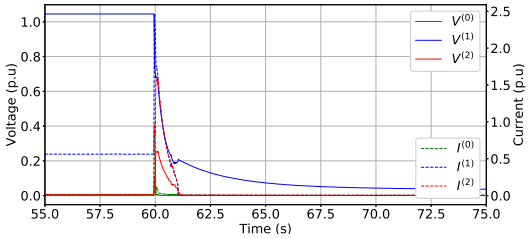

Figure 5. Detail of a real record of a forced shutdown due to a fault at the THVS.

both classifiers had lower accuracy levels (around 50%) for certain classes. In real record scenarios, the fuzzy classifier outperformed the CNN classifier. The lower performance of the CNN classifier was attributed to the disparity between simulated training data and real data. It should be noted that the CNN structure and hyperparameters were not optimized in this study, but the authors acknowledge that optimization could result in improved performance. Nonetheless, the overall results were considered satisfactory.

The two classifiers were proposed to explore different approaches and their requirements. The CNN classifier requires complex data preprocessing, while the fuzzy classifier relies on knowledge about event characteristics. The CNN classifier demands expertise in network structure, layer types, and hyperparameters, affecting training and results. Increasing outputs in the fuzzy classifier adds complexity, whereas the CNN classifier can easily handle more output classes with available data. However, the CNN requires a larger dataset compared to the fuzzy classifier, which relies on specialist knowledge. Fuzzy classifiers are suitable with limited data or uncertainty, but as PMU use expands and more data is available, CNN classifiers become more viable for specific classification.

REFERENCES

Agrawal, R. and Koley, E. (2016). Fuzzy logic based protection scheme for symmetrical and unsymmetrical faults in three phase series compensated transmission line. In *International Conference on Micro-Electronics and Telecommunication Engineering (ICMETE)*.

Asman, S.H., Ab Aziz, N.F., Abd Kadir, M.Z.A., and Amirulddin, U.A.U. (2020). Fault signature analysis based on digital fault recorder in malaysia overhead line system. In *IEEE International Conference on Power and Energy*, 188–193.

Belagoune, S., Bali, N., Bakdi, A., Baadji, B., and Atif, K. (2021). Deep learning through lstm classification and regression for transmission line fault detection, diagnosis and location in large-scale multi-machine power systems. *Measurement*, 177, 109330.

Chen, K., Hu, J., and He, J. (2016). Detection and classification of transmission line faults based on unsupervised feature learning and convolutional sparse autoencoder. *IEEE Transactions on Smart Grid*, 9(3), 1748–1758.

Goodfellow, I., Bengio, Y., and Courville, A. (2016). *Deep Learning*. MIT Press.

Katyara, S., Akhtar, F., Solanki, S., Leonowicz, Z., and Staszewski, L. (2018). Adaptive fault classification approach using digitized fuzzy logic (dfl) based on sequence components. In *IEEE International Conference on Environment and Electrical Engineering*.

Kundur, P. (1994). *Power System Stability and Control*. McGraw-Hill, Inc.

Miranda, V., Cardoso, P.A., Bessa, R.J., and Decker, I. (2019). Through the looking glass: Seeing events in power systems dynamics. *International Journal of Electrical Power & Energy Systems*, 106.

Moreto, M. and Rolim, J.G. (2015). Using disturbance records to automate the diagnosis of faults and operational procedures in power generators. *IET Generation, Transmission & Distribution*, 9(15).

Perez, J. (2010). A guide to digital fault recording event analysis. In *Annual Conference for Protective Relay Engineers*.

Ross, T.J. (2010). *Fuzzy Logic with Engineering Applications*. John Wiley & Sons, Ltd.

Saadat, H. (1999). *Power System Analysis*. McGraw-Hill, Inc.

Wang, W., Yin, H., Chen, C., Till, A., Yao, W., Deng, X., and Liu, Y. (2020). Frequency disturbance event

detection based on synchrophasors and deep learning. *IEEE Transactions on Smart Grid*, 11(4).